DNA AND CELL BIOLOGY
Volume 34, Number 11, 2015

Pp. 669–676
DOI: 10.1089/dna.2015.2959

Activation of SphK1 by K6PC-5 Inhibits Oxygen–Glucose Deprivation/Reoxygenation-Induced Myocardial Cell Death

Jun-jie Shao,[1] Yi Peng,[2] Li-ming Wang,[1] Jian-kai Wang,[1] and Xin Chen[1]

In the current study, we evaluated the potential effect of a novel sphingosine kinase 1 (SphK1) activator, K6PC-5, on oxygen–glucose deprivation (OGD)/reoxygenation-induced damages to myocardial cells. We demonstrated that K6PC-5 increased intracellular sphingosine-1-phosphate (S1P) content and remarkably inhibited OGD/reoxygenation-induced death of myocardial cells (H9c2/HL-1 lines and primary murine myocardiocytes). SphK1 inhibitors, B-5354c and SKI-II, or SphK1-siRNA knockdown not only aggregated OGD/reoxygenation-induced cytotoxicity but also nullified the cytoprotection by K6PC-5. On the other hand, overexpression of SphK1 alleviated H9c2 cell death by OGD/reoxygenation, and K6PC-5-mediated cytoprotection was also enhanced in SphK1 overexpressed cells. Molecularly, OGD/reoxygenation activated the mitochondrial death pathway, evidenced by reactive oxygen species (ROS) production, mitochondrial membrane potential reduction, and p53-cyclophilin D (Cyp-D) association, which were all alleviated by K6PC-5 or overexpression of SphK1, but exacerbated by SphK1 knockdown. Furthermore, OGD/reoxygenation induced prodeath ceramide production in myocardial cells, which was largely suppressed by K6PC-5. In the meantime, adding a cell-permeable short-chain ceramide (C6) mimicked OGD/reoxygenation actions and induced ROS production and the mitochondrial death pathway in myocardial cells. Together, we conclude that K6PC-5 inhibits OGD/reoxygenation-induced myocardial cell death probably through activating SphK1. The results of the study indicate a potential benefit of K6PC-5 on ischemic heart disease.

Introduction

Ischemic heart disease is one of the most common cardiovascular diseases (CVDs) and it is also a major health threat and an important contributor of human mortality in China and around the world (Nabel and Braunwald, 2012; Steptoe and Kivimaki, 2012). In the meantime, its incidence has been steadily increasing in Western and Eastern countries (Nabel and Braunwald, 2012; Steptoe and Kivimaki, 2012). Thus, understanding the associated pathological mechanisms and developing possible intervention strategies are extremely important (Nabel and Braunwald, 2012; Steptoe and Kivimaki, 2012).

Cultured myocardiocytes were often subjected to oxygen–glucose deprivation (OGD) to mimic a cellular model of ischemic heart damage (Ekhterae *et al.*, 1999; Persky *et al.*, 2000; Marambio *et al.*, 2010). Served and/or sustained OGD (>1 h) is shown to disrupt mitochondrial functions through block complex-I activity, and when coupling with reoxygenation, superoxide and other reactive oxygen species (ROS) will be produced, causing oxidative stress and cardiomyocyte necrosis (Ekhterae *et al.*, 1999; Persky *et al.*, 2000; Marambio *et al.*, 2010). However, the detailed mechanisms need further characterizations.

Sphingolipid metabolites, including ceramide, sphingosine, and sphingosine-1-phosphate (S1P), are the new family of lipid messengers (Mullen and Obeid, 2012). The lipid kinase, sphingosine kinase 1 (SphK1), catalyzes the phosphorylation of sphingosine to S1P (Shida *et al.*, 2008; Vadas *et al.*, 2008). *In vivo* and *in vitro* studies have shown that activation of SphK1 is closely linked to cell survival and growth (Shida *et al.*, 2008; Vadas *et al.*, 2008). On the other hand, SphK1 inhibition will lead to sphingosine and ceramide accumulation, causing cell death and apoptosis (Shida *et al.*, 2008; Vadas *et al.*, 2008). The potential role of SphK1 in OGD/reoxygenation-induced death of myocardiocytes and the associated mechanisms have not been extensively studied.

Recent studies have identified a novel and specific SphK1 activator, named K6PC-5 [*N*-(1,3-dihydroxyisopropyl)-2-hexyl-3-oxo-decanamide] (Kwon *et al.*, 2007; Hong *et al.*,

[1]Department of Cardiothoracic Surgery, Nanjing First Hospital, Nanjing, China.
[2]Department of Radiation and Medical Oncology, Hubei Key Laboratory of Tumor Biological Behaviors, Zhongnan Hospital of Wuhan University, Wuhan, China.

2008). This hydrophobic SphK1 activator contains a ketone group, two hydroxy groups, two short alkyl groups, and an amide linkage and it is able to potently and specifically activate SphK1 (Kwon *et al.*, 2007; Hong *et al.*, 2008). In the current study, we show that K6PC-5 inhibits OGD/reoxygenation-induced myocardial cell damages through activation of SphK1 signaling.

Material and Methods

Reagents and antibodies

K6PC-5 was a gift from Dr. Cao Xiaojian's group at Nanjing Medical University (Ji *et al.*, 2015). Antibodies against cyclophilin D (Cyp-D), SphK1, and p53 were obtained from Santa Cruz Biotechnology, Inc. (Santa Cruz, CA). The SphK1 inhibitor, B-5354c, and monoclonal anti-β-actin antibody were purchased from Sigma (St. Louis, MO). SKI-II was obtained from Tocris Bioscience (Ellisville, MO). C6-Ceramide was purchased from Avanti (Alabaster, AB).

Cell culture

As reported (Chen *et al.*, 2011, 2013), rat embryonic ventricular H9c2 myocardiocytes [a gift from Dr. Jiang Lai's group (Chen *et al.*, 2013)] were maintained in Dulbecco's modified Eagle's medium (DMEM), supplemented with a 10% fetal bovine serum (FBS), penicillin/streptomycin, and 4 mM L-glutamine, in a CO_2 incubator at 37°C. HL-1, a murine cell line of myocardiocytes, was purchased from the Cell Bank of Shanghai Institute of Biological Science (Shanghai, China). HL-1 cells were cultured at 37°C in the presence of 7.5% CO_2 according to the instructions in White *et al.* (2004) without adding penicillin/streptomycin.

Murine myocardiocyte isolation and primary culture

Primary murine myocardiocytes were isolated and cultured as described previously (Ito *et al.*, 1991; Simmons *et al.*, 1996). Briefly, ventricles of C57BL6 mice born within 24 h were minced in Hank's balance solution. Myocardiocytes were digested in 0.625 mg/mL collagenase (Sigma) and incubated at 37°C for 40–60 min. The cell suspension was filtered and centrifuged to obtain the cell pellet. Cells were then suspended in M-199 medium supplemented with 5% FBS and 5 mM D-glucose and plated for 40 min to remove nonmyocardiocytes. The myocardiocytes were then plated at a density of 2×10^6 cells/mL in M-199 supplemented with 10% FBS. A confluent monolayer of spontaneously beating cells was formed within 2 days.

OGD/reoxygenation model

As reported (Zheng *et al.*, 2014), H9c2 cells or primary murine myocardiocytes were placed in an anaerobic chamber (HERA cell 150, partial oxygen pressure was maintained below 2 mm Hg) and incubated in glucose-free balanced salt solution (116 mM NaCl, 5.4 mM KCl, 0.8 mM $MgSO_4$, 1.0 mM NaH_2PO_4, 1.8 mM $CaCl_2$, 26.2 mM $NaHCO_3$, 0.025 mM phenol red, and 20 mM sucrose). The solution was bubbled with an anaerobic gas mix (95% N_2, 5% CO_2). Cell cultures subjected to OGD were incubated in the solution at 37°C for 3 h to produce oxygen deprivation and then reoxygenated (returned to the normal aerobic environment). Experimental parameters were assayed following reoxygenation.

Cell viability assay

Cell viability was measured by the 3-[4,5-dimethylthiazol-2-yl]-2,5 diphenyltetrazolium bromide (MTT; Sigma) method. Briefly, cells were seeded onto 96-well plates at a density of 3×10^4 cells/mL. Twenty-four hours after OGD, MTT tetrazolium salt (0.25 mg/mL) was added to each well and incubated in a CO_2 incubator for 2 h at 37°C, 150 μL of dimethyl sulfoxide was then added to dissolve formazan crystals, and the absorbance at 570 nm was measured using a multiwell plate spectrophotometer (Synergy HT; BioTek Instruments, Inc., Shanghai, China). OD values of the treatment group were always normalized to that of the untreated control group.

Trypan blue staining assay

Twenty-four hours after OGD, the percentage (%) of dead cells was calculated by the number of the trypan blue-stained cells/the total cell number × 100%, which was automatically recorded by a handheld automated cell counter (Merck Millipore, Shanghai, China).

Lactate dehydrogenase detection

Cell death was also detected by lactate dehydrogenase (LDH) assay. Briefly, 24 h after OGD/reoxygenation, the content of LDH in the culture medium was analyzed by a two-step enzymatic reaction LDH assay kit (Takara, Tokyo, Japan). The percentage of released LDH was calculated by the following formula: LDH released in conditional medium/(LDH released in conditional medium + LDH in cell lysates) × 100%.

Measurement of S1P content

H9c2/HL-1 cells or the primary murine myocardiocytes were treated with K6PC-5 (0.1–10 μM) for 3 h, cells were then scraped in SphK1 assay buffer described in Ji *et al.* (2015). A 100 μg portion of cell extracts in 185 μL volume was mixed with 5 μL of [γ-32P]ATP (5 μCi; Sigma) containing 0.2 M $MgCl_2$ and 10 μL of 1 mM sphingosine (dissolved in 5% Triton X-100; Sigma), and then incubated for 30 min at 37°C. The reaction was terminated with 10 μL of 1 N HCl. A 400 μL portion of chloroform/methanol/HCl (100:200:1 [v/v]) mixture was added and mixed with the reaction. Then, 120 μL of chloroform and 120 μL of 2 M KCl were added, and phases were separated by centrifugation. The organic phase was dried and resolved by thin-layer chromatography on silica gel G60 with SphK1-butanol/methanol/acetic acid/water (80:20:10:20 [v/v]) (Ji *et al.*, 2015). The radioactive spots corresponding to S1P were detected using filmless autoradiographic analysis (BAS-1500; Fujifilm Co., Ltd., Tokyo, Japan). Total gray was quantified and normalized to that of the untreated control group.

Western blots

Cells were incubated with the lysis buffer containing 50 mM HEPES, 150 mM NaCl, 1 mM EDTA, 1 mM EGTA, 10% glycerol, 0.5% NP-40, 0.5% Tween 20, 1 mM dithiothreitol, and protease inhibitor cocktail (Roche Diagnostics, Indianapolis, IN); Proteins (40 μg/sample) were resolved by sodium dodecyl sulfate–polyacrylamide gel electrophoresis

(SDS-PAGE) and transferred to polyvinylidene fluoride membranes. The latter were incubated sequentially in tris-buffered saline containing 0.05% Tween-20 and 5% nonfat dry milk as follows: no addition, 1 h at room temperature (blocking); primary antibody, overnight at 4°C; and secondary antibody (Amersham), 2 h at room temperature. Bound secondary antibody was detected by the electrochemiluminescence system. Western blot results were quantified by ImageJ software from NIH website.

Mitochondrial immunoprecipitation

As reported (Zheng *et al.*, 2014), 2 h after OGD, mitochondria of 5×10^6 H9c2 cells were isolated using the Mitochondria Isolation Kit for Cultured Cells from Thermo Scientific (Hudson, NH). The mitochondria were then lysed with lysis buffer (20 mM Tris, pH 7.4, 135 mM NaCl, 1.5 mM $MgCl_2$, 1 mM EGTA, 10% glycerol, and 1% Triton X-100). Immunoprecipitation was performed using anti-Cyp-D (Vaseva *et al.*, 2012), and immune complexes were captured with protein A/G-Sepharose (Sigma). Proteins were resolved by SDS-PAGE, and p53-Cyp-D association was detected by the Western blots.

Generation of SphK1 knockdown stable H9c2 cells by lentiviral infection

Two lentiviral shRNAs (−1/−2) against SphK1 were designed, verified, and provided by Nanjing Keygen Biotech (Nanjing, China). H9c2 cells were seeded onto a six-well plate with 50–60% of confluence, 20 μL/mL of SphK1 shRNA containing lentiviral particles was added, and cells were cultured for additional 24 h. Cell culture medium was replaced with fresh puromycin (0.5 μg/mL; Sigma)-containing medium every 2 days to select resistant colonies. The expression of SphK1 was detected by Western blots in the resistant colonies. Control H9c2 cells were infected with scramble control shRNA (sc-shRNA) lentivirus.

SphK1 overexpression in H9c2 cells

A SphK1-flag pLKO.1 lentiviral construct was a gift from Dr. Zhangping Gu (Yao *et al.*, 2012). H9c2 cells were seeded onto a six-well plate with 50–60% of confluence, 20 μL/mL of SphK1 construct was added, and cells were cultured for additional 24 h. Cell culture medium was replaced with fresh puromycin (0.5 μg/mL)-containing medium every 2 days to select resistant colonies. Control cells were infected with empty vector (pLKO.1) lentiviral construct (Yao *et al.*, 2012).

ROS detection

Three to 6 h after OGD, H9c2 cells or primary murine myocardiocytes were incubated with 5 μM carboxy-H2-DCFDA (Molecular Probes, Shanghai, China). The percent of fluorescence-positive cells as a measure of ROS generation was recorded under a fluorescent microplate reader (PLX 800; BioTek Instruments, Inc.) using excitation and emission filters of 488 and 530 nm, respectively.

Detection of mitochondrial membrane potential

Mitochondrial membrane potential (MMP) was measured through JC-10 dye (Invitrogen, Carlsbad, CA) (Zhen *et al.*, 2014). The JC-10 dye exhibits two staining spectra. In normally resting cells, the dye forms aggregates in the mitochondrial membrane, exhibiting orange fluorescence. When the membrane potential is decreasing, the monomeric JC-10 will form in the cytosol, exhibiting green fluorescence. Thus, green fluorescence was detected as an indicator of MMP reduction. Three to 6 h after OGD, H9c2 cells were incubated with 10 μg/mL of JC-10 for 5 min at room temperature in the dark. Cells were then washed twice with warm phosphate-buffered saline and tested under a fluorescent microplate reader (PLX 800; BioTek Instruments, Inc.) using excitation and emission filters of 488 and 530 nm, respectively.

Measurement of cellular ceramide

The cellular ceramide production was analyzed with the help from Dr. Cao Xiaojian's group at Nanjing Medical University [see protocol in Ji *et al.* (2015)]. The level of ceramide in the treatment group was normalized to that of the untreated control group.

Statistical analysis

Data are expressed as mean ± standard deviation (SD), multiple group comparison was performed by one-way analysis of variance (ANOVA), followed by the least significant difference procedure for comparison of means. Comparison between two groups under identical conditions was performed by the two-tailed Student's *t*-test (Excel). A value of $p < 0.05$ was considered statistically significant.

Results

K6PC-5 inhibits OGD/reoxygenation-induced death of myocardial cells

At first, myocardial H9c2 cells were treated with applied concentrations of K6PC-5; MTT cell viability results demonstrated that K6PC-5 was noncytotoxic to H9c2 cells, except at a high concentration (25 μM) (Fig. 1A). Since K6PC-5 is a newly identified SphK1 activator, its effect on S1P production was tested. Results in Figure 1B showed that K6PC-5 dose-dependently increased the intracellular S1P content in H9c2 cells, suggesting SphK1 activation. S1P is a well-known myocardial protectant (Karliner *et al.*, 2001; Jin *et al.*, 2002). We then tested the potential role of K6PC-5 on OGD/reoxygenation-induced myocardial cell death. H9c2 cells were subjected to OGD for 3 h, followed by reoxygenation for additional 24 h. OGD/reoxygenation induced significant H9c2 cell death, which was evidenced by decreased cell viability (Fig. 1C), increased trypan blue staining (Fig. 1D), and LDH release to the conditional medium (Fig. 1E). Importantly, pretreatment with K6PC-5 at 1/10 μM remarkably inhibited OGD/reoxygenation-induced H9c2 cell death (Fig. 1C–E). Significantly, the intracellular S1P content was also increased in K6PC-5-treated HL-1 and primary murine myocardiocytes (Fig. 1F). The potential cytoprotective effect of K6PC-5 in these murine myocardiocytes was also tested. Results demonstrated that K6PC-5 (10 μM) pretreatment significantly inhibited OGD/reoxygenation-induced cytotoxicity in HL-1 (Fig. 1G) and primary murine myocardiocytes (Fig. 1H, I). Note that K6PC-5 alone (10 μM) had no significant effect on the survival of the murine myocardiocytes (Fig. 1G–I). Together, these results clearly showed that K6PC-5 protected myocardial cells from OGD/reoxygenation.

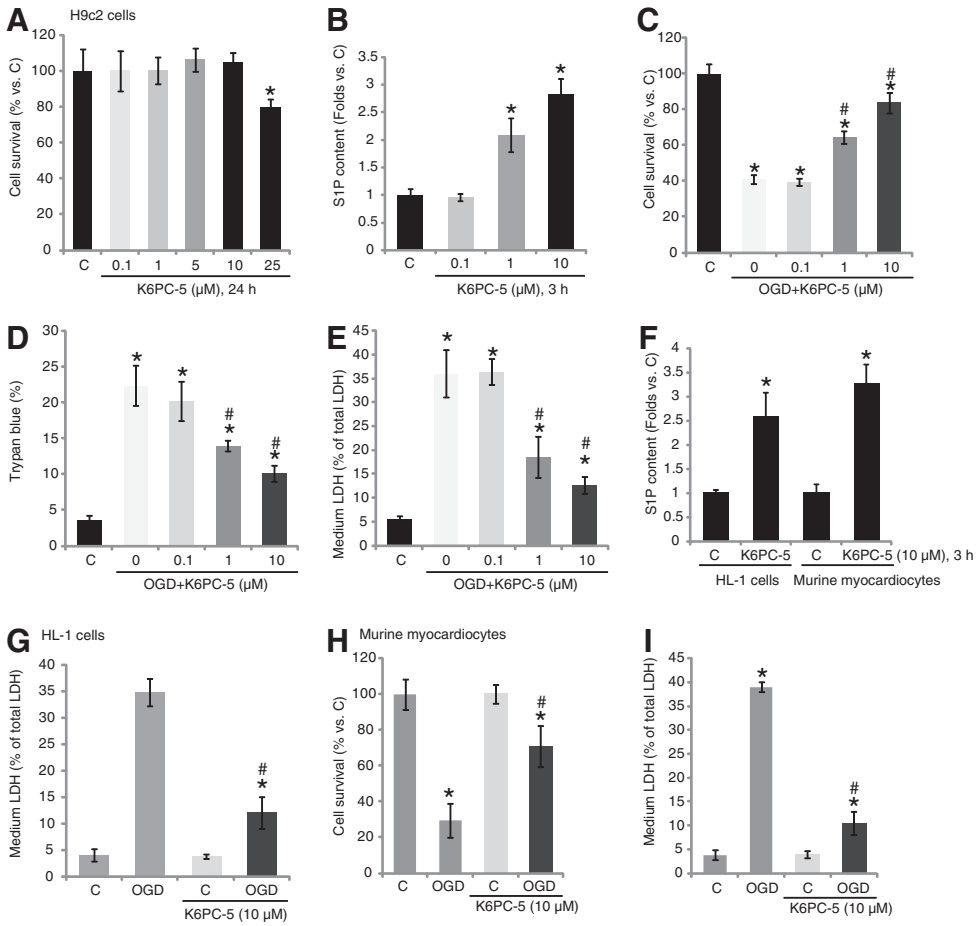

FIG. 1. K6PC-5 inhibits OGD/reoxygenation-induced myocardial cell death. H9c2 cells were treated with applied concentrations of K6PC-5 (0–25 μM); after 24 h, cell viability was tested by MTT assay **(A)**, and the intracellular S1P content was tested after 3 h **(B)**. H9c2 cells, pretreated with applied concentrations of K6PC-5 (0.1–10 μM, 1-h pretreatment), were maintained under OGD for 3 h, followed by 24 h of reoxygenation. MTT assay **(C)**, trypan blue staining assay **(D)**, and LDH release assay **(E)** were then performed to test cell survival and cell death. HL-1 or primary murine myocardiocytes were treated with K6PC-5 (10 μM) for 3 h, and S1P content was tested **(F)**. HL-1 **(G)** or primary murine myocardiocytes **(H, I)** were pretreated with K6PC-5 (10 μM) for 1 h, followed by the OGD/reoxygenation procedure; cell viability and cell death were tested similarly. ''C'' stands for untreated control (Same for all Figures). ''OGD'' stands for OGD/reoxygenation (Same for all Figures). Bars indicate SD. Each experiment was repeated thrice and similar results were obtained. $^{*}p < 0.05$ versus group C. $^{\#}p < 0.05$ versus OGD/reoxygenation only group. LDH, lactate dehydrogenase; MTT, 3-[4,5-dimethylthiazol-2-yl]-2,5 diphenyltetrazolium bromide; OGD, oxygen–glucose deprivation; S1P, sphingosine-1-phosphate; SD, standard deviation.

SphK1 participates in OGD/reoxygenation-induced myocardial cell death

The results above demonstrated that K6PC-5, the novel SphK1 activator (Hong *et al.*, 2008; Ji *et al.*, 2015), is cytoprotective against OGD/reoxygenation. Next, we tested the involvement of SphK1 in OGD/reoxygenation-mediated cell death. As described, H9c2 cells were infected with SphK1 shRNA (–1/–2) containing lentivirus. Through the Western blot assay, we showed that SphK1 was dramatically downregulated in the stable cells bearing SphK1 shRNA (Fig. 2A). Both shRNA showed remarkable efficiency, resulting in over 80% of downregulation of SphK1 in H9c2 cells (Fig. 2A). Significantly, SphK1 silencing increased OGD/reoxygenation-induced H9c2 cytotoxicity (Fig. 2B, C), indicating a role of SphK1 in OGD-mediated cell death. Furthermore, B-5354c (Kono *et al.*, 2002) and SKI-II (Chiba *et al.*, 2010; Li *et al.*, 2014), two established SphK1 inhibitors, similarly aggravated H9c2 cell death by OGD/reoxygenation (Fig. 2D). To further confirm the role of SphK1 in OGD/reoxygenation-induced cell death, a wild-type SphK1-flag was introduced to H9c2 cells, and stable cells were established. Western blot assay confirmed SphK1 overexpression in cells with the construct (wt-SphK1-flag) (Fig. 2E). Notably, OGD/reoxygenation-mediated H9c2 cell death was alleviated in SphK1 overexpressed cells (Fig. 2F). In primary murine myocardiocytes, MTT results showed that B-5354c and SKI-II enhanced cell death by OGD/reoxygenation (Fig. 2G). Together, these results suggest that SphK1 is involved in OGD/reoxygenation-induced myocardial cell death.

K6PC-5-mediated cytoprotection against OGD/reoxygenation requires SphK1 activation

Next, we studied whether K6PC-5-mediated activity in myocardial cells is through activation of SphK1. Using the

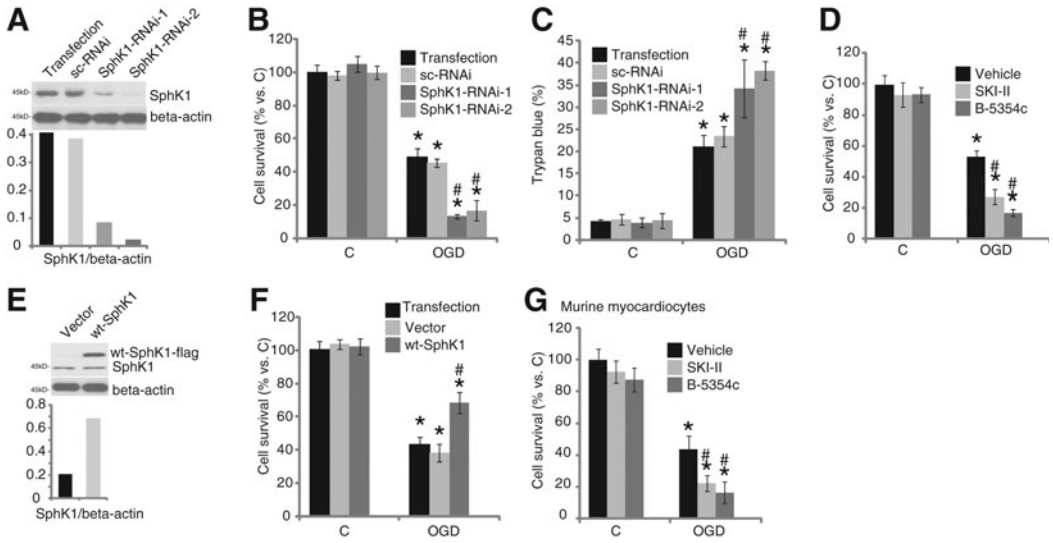

FIG. 2. SphK1 is involved in OGD/reoxygenation-induced myocardial cell death. Stable H9c2 cells bearing indicated construct (scramble control shRNA [sc-RNAi], SphK1 shRNA-1 [SphK1-RNAi-1], SphK1 shRNA-2 [SphK1-RNAi-2], empty vector [pLKO.1], or wt-SphK1-flag) were maintained under OGD for 3 h, followed by 24 h of reoxygenation; SphK1 and β-actin expression was tested by Western blots **(A, E)**; cell survival and cell death were tested by MTT assay **(B, F)** and trypan blue staining assay **(C**, for H9c2 cells**)**, respectively. H9c2 cells or primary murine myocardiocytes, pretreated with B-5354c (10 μM), SKI-II (10 μM), or vehicle (0.1% DMSO) for 1 h, were then subjected to OGD/reoxygenation; after 24 h, cell viability was tested **(D, G)**. ''Transfection'' stands for empty lentiviral particles (Same for all figures). Bars indicate SD. Each experiment was repeated thrice and similar results were obtained. $^{*}p < 0.05$ versus group C. $^{\#}p < 0.05$ versus OGD/reoxygenation only group. DMSO, dimethyl sulfoxide; SphK1, sphingosine kinase 1.

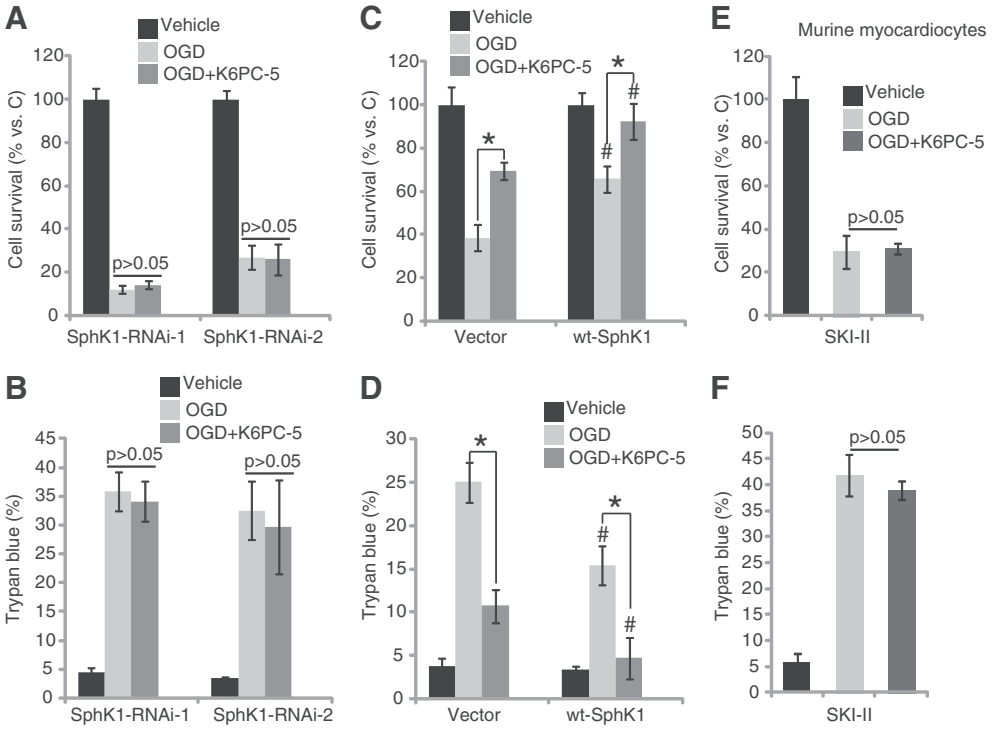

FIG. 3. K6PC-5-mediated cytoprotection against OGD/reoxygenation requires SphK1 activation. Stable H9c2 cells bearing indicated construct (SphK1 shRNA-1 [SphK1-RNAi-1], SphK1 shRNA-2 [SphK1-RNAi-2], empty vector [pLKO.1], or wt-SphK1-flag) were pretreated with K6PC-5 (10 μM), followed by OGD/reoxygenation after 24 h; cell viability **(A, C)** and cell death **(B, D)** were tested. Murine myocardiocytes were pretreated with SKI-II (10 μM) or plus K6PC-5 (10 μM), followed by OGD/reoxygenation; after 24 h, cell viability **(E)** and cell death **(F)** were tested. Bars indicate SD. Each experiment was repeated thrice and similar results were obtained. $^{*}p < 0.05$ versus group C. $^{\#}p < 0.05$ versus the Vector group (for **C, D**).

same methods described in Figure 2, we showed that K6PC-5-mediated protection against OGD/reoxygenation was almost completely nullified in H9c2 cells depleted with SphK1 (Fig. 3A, B). In other words, K6PC-5 was not effective in SphK1-silenced stable H9c2 cells (Fig. 3A, B). On the other hand, when we overexpressed SphK1 in H9c2 cells, K6PC-5-mediated cytoprotection was enhanced (Fig. 3C, D). As a matter of fact, K6PC-5 almost completely blocked OGD/reoxygenation-induced cytotoxicity in SphK1 overexpressed H9c2 cells (Fig. 3C, D). In primary murine myocardiocytes, SKI-II pretreatment also abolished K6PC-5-mediated cytoprotection (Fig. 3E, F). Together, these results indicate that K6PC-5 induces cytoprotection in myocardial cells possibly through activating SphK1.

K6PC-5 inhibits the OGD/reoxygenation-induced mitochondrial death pathway in myocardial cells

Recent studies have explored the role of the mitochondrial death pathway in OGD/reoxygenation-induced damages to myocardial cells (Zheng *et al.*, 2014). Zheng *et al.* (2014) showed that OGD/reoxygenation induces ROS production, causing p53 mitochondrial translocation and Cyp-D complexation. The latter mediates mitochondrial permeability transition pore (mPTP) opening following cell necrosis (Zheng *et al.*, 2014). Consistent with these findings, we also observed ROS production (Fig. 4A), MMP reduction (indicator of mPTP opening, Fig. 4B), and Cyp-D-p53 mitochondrial association (Fig. 4C) in OGD/reoxygenation-stimulated H9c2 cells. Significantly, pretreatment with K6PC-5 remarkably inhibited these changes by OGD/reoxygenation (Fig. 4A–C). Furthermore, we provided evidence to show that SphK1 might be involved in OGD/reoxygenation-induced activation of the mitochondrial death pathway. Knockdown of SphK1 by shRNA enhanced OGD/reoxygenation-induced MMP reduction in H9c2 cells (Fig. 4D). On the other hand, overexpression of SphK1 inhibited MMP loss by OGD (Fig. 4D). In primary murine myocardiocytes, OGD/reoxygenation-induced MMP reduction was again inhibited by K6PC-5, but was exacerbated by the SphK1 inhibitor B-5354c or SKI-II (Fig. 4E). Together,

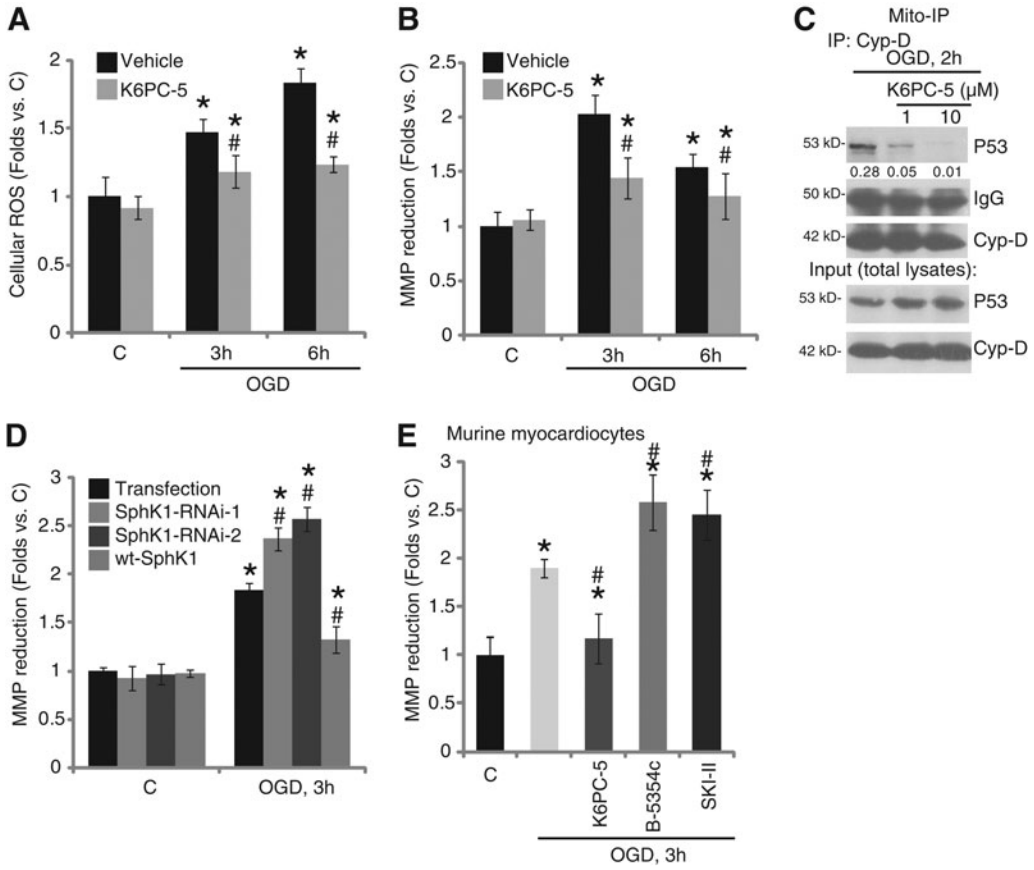

FIG. 4. K6PC-5 inhibits the OGD/reoxygenation-induced mitochondrial death pathway in myocardial cells. H9c2 cells were pretreated with K6PC-5 (1/10 μM), followed by OGD/reoxygenation; cellular ROS production **(A)** and MMP reduction **(B)** were tested; the association between p53 and Cyp-D in mitochondria was also tested by Mito-IP **(C)**; Cyp-D-bound P53 was quantified **(C)**. Stable H9c2 cells with SphK1 shRNA (−1/ −2) or wt-SphK1 cDNA were subjected to OGD/reoxygenation; MMP reduction was tested by JC-10 dye assay **(D)**. Primary murine myocardiocytes were pretreated with K6PC-5 (10 μM), B-5354c (10 μM), or SKI-II (10 μM), cells were then subjected to OGD/reoxygenation, and MMP reduction was tested **(E)**. Bars indicate SD. Each experiment was repeated thrice and similar results were obtained. $^{*}p < 0.05$ versus group C. $^{\#}p < 0.05$ versus OGD/reoxygenation only group. Cyp-D, cyclophilin D; Mito-IP, mitochondrial immunoprecipitation; MMP, mitochondrial membrane potential; ROS, reactive oxygen species.

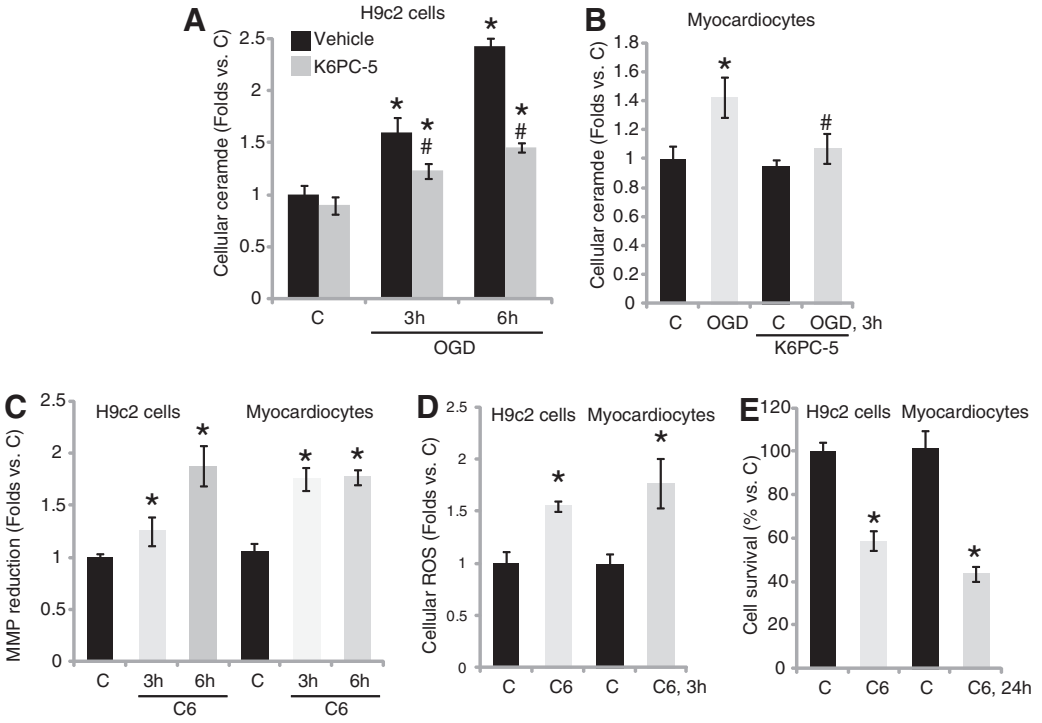

FIG. 5. OGD/reoxygenation induces prodeath ceramide production inhibited by K6PC-5. H9c2 cells or primary murine myocardiocytes were pretreated with K6PC-5 (10 μM), followed by OGD/reoxygenation; the cellular ceramide level was tested **(A, B)**. H9c2 cells were treated with C6 ceramide (25 μM) for the indicated time; MMP reduction **(C)**, ROS level **(D)**, and cell survival **(E)** were tested as mentioned. Each experiment was repeated thrice and similar results were obtained. $^{*}p < 0.05$ versus group C. $^{\#}p < 0.05$ versus OGD/reoxygenation only group **(A, B)**.

we suggest that activation of SphK1 by K6PC-5 inhibits the OGD/reoxygenation-induced mitochondrial death pathway in myocardial cells.

OGD/reoxygenation induces prodeath ceramide production inhibited by K6PC-5

To further understand the underlying mechanisms of OGD/reoxygenation-induced death of myocardial cells, the involvement of ceramide was tested. As shown in Figure 5A and B, OGD/reoxygenation induced significant ceramide production in H9c2 cells and in primary murine myocardiocytes. Remarkably, pretreatment with K6PC-5 largely inhibited ceramide accumulation by OGD/reoxygenation (Fig. 5A, B). To connect these findings with previous results, we found that adding a cellular permeable ceramide (C6) also induced MMP reduction (Fig. 5C), ROS production (Fig. 5D), and death (Fig. 5E) in both H9c2 cells and in primary murine myocardiocytes. Based on this information, we propose that OGD/reoxygenation induces ceramide production, which possibly mediates oxidative stress and activation of the mitochondrial death pathway. K6PC-5 activates SphK1, thus inhibiting ceramide production and myocardial cell death.

Discussions

Ischemic heart diseases are among the most lethal CVDs, causing significant mortality around the world. OGD/reoxygenation is often applied in cultured myocardial cells to mimic ischemic–reperfusion damage and to explore the underlying mechanisms and screen potential intervention methods (Ekhterae *et al.*, 1999; Persky *et al.*, 2000; Marambio *et al.*, 2010). Our results here demonstrated that K6PC-5, the novel SphK1 activator, remarkably inhibited OGD/reoxygenation-induced myocardial cell death through activation of SphK1. SphK1 inhibition or silencing not only aggregated OGD/reoxygenation's cytotoxicity but also nullified the cytoprotection by K6PC-5. On the other hand, overexpression of SphK1 alleviated H9c2 cell death by OGD/reoxygenation, and K6PC-5-mediated cytoprotection was also enhanced in SphK1 overexpressed cells.

Recent studies have explored the signaling mechanisms of cell necrosis by OGD/reoxygenation. OGD/reoxygenation was shown to induce cytoplasmic p53 translocation to the inner mitochondrial membrane, where it forms a complex with the local protein, Cyp-D (Baumann, 2012; Karch and Molkentin, 2012; Vaseva *et al.*, 2012; Zheng *et al.*, 2014). The complexation is required for subsequent mPTP opening and subsequent cell necrosis (Zheng *et al.*, 2014). Inhibition of this complexation by Cyp-D inhibitors or by p53/Cyp-D deficiency significantly suppressed cell necrosis by OGD/reoxygenation (Zheng *et al.*, 2014). In the current study, we showed that ceramide production could be a possible upstream signaling for this mitochondrial death pathway after OGD/reoxygenation, although the detailed mechanisms still need investigations.

We demonstrated that OGD/reoxygenation-induced ceramide production and mitochondrial death pathway activation were both inhibited by K6PC-5, while exogenously added C6 ceramide mimicked OGD/reoxygenation's actions and activated the mitochondrial death pathway in myocardial cells.

Thus, we suggest that OGD/reoxygenation induces ceramide production, which activates the mitochondrial death pathway to promote myocardial cell death. SphK1 activation by K6PC-5 inhibits ceramide production and thus protects myocardial cells from OGD/reoxygenation. More studies are needed to understand the insights of this link.

Conclusions

In summary, the results of this study indicate that K6PC-5 potently inhibits OGD/reoxygenation-induced myocardial cell death through activating SphK1 signaling. It might be worth testing this novel SphK1 activator in an animal model of ischemic heart damage.

Acknowledgment

This work was supported by the National Natural Science Foundation of China.

Disclosure Statement

No competing financial interests exist.

References

Baumann, K. (2012). Cell death: multitasking p53 promotes necrosis. Nat Rev Mol Cell Biol **13,** 480–481.

Chen, M.B., *et al.* (2011). Activation of AMP-activated protein kinase contributes to doxorubicin-induced cell death and apoptosis in cultured myocardial H9c2 cells. Cell Biochem Biophys **60,** 311–322.

Chen, Z., *et al.* (2013). TAK1 activates AMPK-dependent cell death pathway in hydrogen peroxide-treated cardiomyocytes, inhibited by heat shock protein-70. Mol Cell Biochem **377,** 35–44.

Chiba, Y., *et al.* (2010). SKI-II, an inhibitor of sphingosine kinase, ameliorates antigen-induced bronchial smooth muscle hyperresponsiveness, but not airway inflammation, in mice. J Pharmacol Sci **114,** 304–310.

Ekhterae, D., *et al.* (1999). ARC inhibits cytochrome c release from mitochondria and protects against hypoxia-induced apoptosis in heart-derived H9c2 cells. Circ Res **85,** e70–e77.

Hong, J.H., *et al.* (2008). K6PC-5, a direct activator of sphingosine kinase 1, promotes epidermal differentiation through intracellular $Ca2^{+}$ signaling. J Invest Dermatol **128,** 2166–2178.

Ito, H., *et al.* (1991). Endothelin-1 induces hypertrophy with enhanced expression of muscle-specific genes in cultured neonatal rat cardiomyocytes. Circ Res **69,** 209–215.

Ji, F., *et al.* (2015). K6PC-5, a novel sphingosine kinase 1 (SphK1) activator, alleviates dexamethasone-induced damages to osteoblasts through activating SphK1-Akt signaling. Biochem Biophys Res Commun **458,** 568–575.

Jin, Z.Q., *et al.* (2002). Cardioprotection mediated by sphingosine-1-phosphate and ganglioside GM-1 in wild-type and PKC epsilon knockout mouse hearts. Am J Physiol Heart Circ Physiol **282,** H1970–H1977.

Karch, J., *et al.* (2012). Is p53 the long-sought molecular trigger for cyclophilin D-regulated mitochondrial permeability transition pore formation and necrosis? Circ Res **111,** 1258–1260.

Karliner, J.S., *et al.* (2001). The lysophospholipids sphingosine-1-phosphate and lysophosphatidic acid enhance survival during hypoxia in neonatal rat cardiac myocytes. J Mol Cell Cardiol **33,** 1713–1717.

Kono, K., *et al.* (2002). Inhibition of recombinant sphingosine kinases by novel inhibitors of microbial origin, F-12509A and B-5354c. J Antibiot (Tokyo) **55,** 99–103.

Kwon, Y.B., *et al.* (2007). Novel synthetic ceramide derivatives increase intracellular calcium levels and promote epidermal keratinocyte differentiation. J Lipid Res **48,** 1936–1943.

Li, P.H., *et al.* (2014). A sphingosine kinase-1 inhibitor, SKI-II, induces growth inhibition and apoptosis in human gastric cancer cells. Asian Pac J Cancer Prev **15,** 10381–10385.

Marambio, P., *et al.* (2010). Glucose deprivation causes oxidative stress and stimulates aggresome formation and autophagy in cultured cardiac myocytes. Biochim Biophys Acta **1802,** 509–518.

Mullen, T.D., *et al.* (2012). Ceramide and apoptosis: exploring the enigmatic connections between sphingolipid metabolism and programmed cell death. Anticancer Agents Med Chem **12,** 340–363.

Nabel, E.G., *et al.* (2012). A tale of coronary artery disease and myocardial infarction. N Engl J Med **366,** 54–63.

Persky, A.M., *et al.* (2000). Protective effect of estrogens against oxidative damage to heart and skeletal muscle in vivo and in vitro. Proc Soc Exp Biol Med **223,** 59–66.

Shida, D., *et al.* (2008). Targeting SphK1 as a new strategy against cancer. Curr Drug Targets **9,** 662–673.

Simmons, W.W., *et al.* (1996). Cytokines and insulin induce cationic amino acid transporter (CAT) expression in cardiac myocytes. Regulation of L-arginine transport and no production by CAT-1, CAT-2A, and CAT-2B. J Biol Chem **271,** 11694–11702.

Steptoe, A., *et al.* (2012). Stress and cardiovascular disease. Nat Rev Cardiol **9,** 360–370.

Vadas, M., *et al.* (2008). The role of sphingosine kinase 1 in cancer: oncogene or non-oncogene addiction? Biochim Biophys Acta **1781,** 442–447.

Vaseva, A.V., *et al.* (2012). p53 opens the mitochondrial permeability transition pore to trigger necrosis. Cell **149,** 1536–1548.

White, S.M., *et al.* (2004). Cardiac physiology at the cellular level: use of cultured HL-1 cardiomyocytes for studies of cardiac muscle cell structure and function. Am J Physiol Heart Circ Physiol **286,** H823–H829.

Yao, C., *et al.* (2012). Co-administration phenoxodiol with doxorubicin synergistically inhibit the activity of sphingosine kinase-1 (SphK1), a potential oncogene of osteosarcoma, to suppress osteosarcoma cell growth both in vivo and in vitro. Mol Oncol **6,** 392–404.

Zhen, Y.F., *et al.* (2014). P53 dependent mitochondrial permeability transition pore opening is required for dexamethasone-induced death of osteoblasts. J Cell Physiol **229,** 1475–1483.

Zheng, K., *et al.* (2014). Salidroside inhibits oxygen glucose deprivation (OGD)/re-oxygenation-induced H9c2 cell necrosis through activating of Akt-Nrf2 signaling. Biochem Biophys Res Commun **451,** 79–85.

Address correspondence to:
Xin Chen, MD, PhD
Department of Cardiothoracic Surgery
Nanjing First Hospital
68 Chang-le Road
Qin-huai District
Nanjing 210029
Jiangsu
China

E-mail: drchenxinnanjing@163.com

Received for publication June 1, 2015; received in revised form July 29, 2015; accepted July 30, 2015.